Human Reidentification with Transferred Metric Learning

Wei Li, Rui Zhao and Xiaogang Wang

Electronic Engineering Department, the Chinese University of Hong Kong

Abstract. Human reidentification is to match persons observed in non-overlapping camera views with visual features for inter-camera tracking. The ambiguity increases with the number of candidates to be distinguished. Simple temporal reasoning can simplify the problem by pruning the candidate set to be matched. Existing approaches adopt a fixed metric for matching all the subjects. Our approach is motivated by the insight that different visual metrics should be optimally learned for different candidate sets. We tackle this problem under a transfer learning framework. Given a large training set, the training samples are selected and reweighted according to their visual similarities with the query sample and its candidate set. A weighted maximum margin metric is online learned and transferred from a generic metric to a candidate-set-specific metric. The whole online reweighting and learning process takes less than two seconds per candidate set. Experiments on the VIPeR dataset and our dataset show that the proposed transferred metric learning significantly outperforms directly matching visual features or using a single generic metric learned from the whole training set.

1 Introduction

Human reidentification has drawn great interest in video surveillance recently [1–4]. It is to match humans observed in non-overlapping camera views based on their visual features and is very important for inter-camera tracking. Human reidentification is a challenging problem, since the same person observed in different camera views undergoes significant changes of resolutions, lightings, poses and viewpoints. Because humans captured by surveillance cameras, especially in far-field video surveillance, are often in small sizes and a lot of their visual details such as facial components are indistinguishable in images, some of them look similar in appearance. The ambiguity increases with the number of persons to be distinguished. Many visual features of characterizing color [5, 6], shape [7, 8] and texture [9–11] of objects have been proposed. In order to overcome the large visual changes across camera views, learning approaches were typically adopted. They learned either the transformations of visual features between camera views [12–15] or visual distance metrics [16–18, 2, 19, 4] from a training set.

In inter-camera tracking, given a query sample observed in a camera view, simple temporal reasoning can be made by roughly estimating the transition time across cameras. Such reasoning can simplify the matching problem by pruning

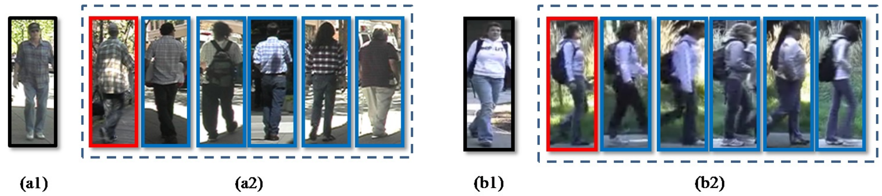

Fig. 1. Examples of query samples and their corresponding candidate sets in human reidentification. (a1) and (b1) are query samples observed in a camera view. (a2) and (b2) are persons in the corresponding candidate sets observed in another camera view after pruning with temporal reasoning. The red windows indicate the truly matched persons. The persons in candidate set (a2) can be well distinguished with color histograms but some of them have similar texture. The persons in candidate set (b2) have similar color histograms. Therefore, distinguishing them has to rely more on other type of features.

the candidate set observed in another camera view. Existing approaches always use the same set of visual features and a fixed distance metric to match any query samples with any candidates, which is not an optimal solution. Since the goal is to distinguish a small number of persons in a particular candidate set, a candidate-set-specific visual metric is preferred. As an example shown in Figure 1, the persons in the first candidate set can be well distinguished with color histograms, while those in the second candidate set are similar in color and other features such as shape and texture could be more effective on them. Unfortunately, each person in the candidate set only has one sample observed in one camera view since the correspondences of samples across camera views are unknown during online tracking, while metric learning requires pairs of samples observed in different camera views with correspondence information. Therefore, directly applying existing metric learning algorithms to obtain a candidate-set-specific metric is infeasible. We tackle this problem under a transfer learning framework. As shown in Figure 2, for each sample in the candidate set, its nearest neighbors in the training set are found by directly matching their visual features. When the training set is large, the found nearest neighbors are likely to be visually similar to the sample in the candidate set and their corresponding training samples in another camera view are known with the ground truth labels. Therefore, the candidate-set-specific metric can be indirectly learned from the selected training pairs. These training pairs are weighted according to their visual similarities to the samples in the candidate set and the query sample. For each candidate set, a metric which maximizes the margin between the correctly matched pairs and wrongly matched pairs is learned [20]. In order to avoid overfitting, the candidate-set-specific metric is regularized by a generic metric learned from the whole training set. To the best of our knowledge, this is the first time for transfer learning to be applied to human reidentification. Experiments on the VIPeR database [21] and our dataset show that it significantly outperforms the approach of directly matching visual features or using a generic distance metric. The weighting and transfer learning process takes less than two seconds per candidate set. It can be applied to both online and offline human reidentification.

Fig. 2. (a) A query sample observed in camera view A. (b) Samples of four candidate persons observed in camera B based on temporal reasoning. (c) The nearest neighbors of each candidate in (b) found from a large training set by directly matching the visual features observed in camera B. Each person in the training set has a pair of samples observed in both cameras A and B according to manually labeled ground truth. Therefore the paired samples of the found nearest neighbors can be used to train the candidate-set-specific metric. Blue windows indicate samples observed in camera A and green windows indicate samples observed in camera B. w_{ij}^A and w_{ij}^B are the weights assigned to training samples according to their visual similarities with the candidates and the query sample respectively. See details in Section 3.2.

2 Related Work

Many approaches have been proposed to learn the distance metrics to match the visual features of image regions observed in different camera views. Schwartz and Davis [2] proposed an approach of projecting high dimensional features to a low dimensional discriminant latent space by Partial Least Squares reduction. It weighted features according to their discriminative power to best distinguish the observations of one object with those of others in the training set in a one-against-all scheme. Lin and Davis [18] learned a different pairwise dissimilarity profile which best distinguished a pair of persons. It was assumed that a feature may be crucial to discriminate two very similar objects but not be effective for other objects. Therefore it is easier to train discriminative features in a pairwise scheme. However, these two approaches required that all the persons to be reidentified have examples in the training set. They can not re-identify a new person. Zheng *et al.* [4] proposed a *Probabilistic Relative Distance Comparison* model. It formulated object reidentification as a distance learning problem and maximized the probability that a pair of true match has a smaller distance than a wrong match pair. In [16, 19] boosting and RankSVM were used to select an optimal subset of features for matching objects across camera views. They could be generalized to persons outside the training set. They targeted on learning a generic metric to distinguish all the persons, which is very challenging since the distribution of visual features from arbitrary persons is very complex. Moreover, any generic metric could be suboptimal for a specific subset of persons whose visual features distribute in some local regions of the high dimensional feature space.

Transfer learning assumes that the distribution of the training data differs from the test data. It automatically adjusts the weights of training samples to match the distributions of training and test data. Various transfer learning algorithms, such as TrAdaBoost [22], weighted margin SVM [23], localized SVM [24] and cross-domain SVM [24] were proposed. Transfer learning has been widely applied to various vision problems such as object recognition [25], object detection [26], image and video retrieval [27], and visual concept classification [28, 24, 29, 30]. In cross-domain SVM [24], each training sample is weighted according to its closeness to the test data. It is related to our approach. However, different than [24], a distance metric instead of a hyperplane is learned in our case. Besides reweighting training samples, our adaptive metric is also regularized by a generic metric. Query-specific distance metric learning [31] optimally distinguishes query person with anyone else in the dataset, while ours optimally distinguish query person with others **ONLY** in the candidate set. So ours is both query-specific and candidate-set-specific which is the most important novelty of this paper.

3 Our Method

3.1 Visual Features

We employ five types of low-level visual features including dense color histograms, dense SIFT [32], HOG [7], Gabor [24] and LBP [10]. They characterize the color distributions, shape and texture of objects. Image regions are normalized to 160×60. For dense color histograms and dense SIFT, a uniform 20×12 grid is placed on the image region, and color histograms in the RGB color space and SIFT descriptors are densely computed on the grid. For each type of features, PCA is applied to retain 90% energy and then each feature vector is normalized to zero mean and unit variance. Different types of features are concatenated to form a single feature vector.

3.2 Searching and weighting training samples

Our approach includes two key steps: searching and weighting nearest training samples for each candidate; and learning an adaptive metric for each candidate set. Let $\mathbf{x}_q^A$ be the visual feature vector of a query sample observed in camera A, and $\mathcal{X}_c^B = \{\mathbf{x}_1^B, \ldots, \mathbf{x}_N^B\}$ be a set of candidates observed in camera view B after pruning with temporal reasoning. For each candidate $\mathbf{x}_i^B$, a set of samples $\tilde{\mathcal{X}}_i^B = \{\tilde{\mathbf{x}}_{i_1}^B, \ldots, \tilde{\mathbf{x}}_{i_{K_i}}^B\}$ close to $\mathbf{x}_i^B$ is selected from the training set $\mathcal{S}$. A straightforward way is to set $\tilde{\mathcal{X}}_i^B$ as the K nearest neighbors of $\mathbf{x}_i^B$ in $\mathcal{S}$ (denoted with $\mathcal{N}_K(\mathbf{x}_i^B)$) by comparing the visual features. However, this approach is not quite stable, since some $\mathbf{x}_i^B$ may be dissimilar with any samples in $\mathcal{S}$. In that case, none of the training samples should be selected and we should rely on the generic metric. We recompute the similarity between $\mathbf{x}_i^B$ and a sample $\tilde{\mathbf{x}}_j^B$ in $\mathcal{S}$ as following,

$$s(\mathbf{x}_i^B, \tilde{\mathbf{x}}_j^B) = \frac{|\mathcal{N}_K(\mathbf{x}_i^B) \cap \mathcal{N}_K(\tilde{\mathbf{x}}_j^B)|}{|\mathcal{N}_K(\mathbf{x}_i^B) \cup \mathcal{N}_K(\tilde{\mathbf{x}}_j^B)|}. \tag{1}$$

The intuition is that if $\mathbf{x}_i^B$ and $\tilde{\mathbf{x}}_j^B$ are visually similar, they should share more nearest neighbors in the training set[1]. $\tilde{\mathcal{X}}_i^B$ is selected by choosing $\tilde{\mathbf{x}}_j^B$ with $s(\mathbf{x}_i^B, \tilde{\mathbf{x}}_j^B) > s_0$, where s_0 is a threshold. $\mathcal{N}_K(\cdot)$ characterizes the geometric structures of the training set. It is more reliable than directly thresholding the visual distance $\|\mathbf{x}_i^B - \tilde{\mathbf{x}}_j^B\|_2^2$, whose value is difficult to be interpreted and whose threshold is hard to be decided. The nearest neighbors of training samples can be pre-computed offline and a reverse mapping maintains the neighbors of each sample. After $\mathcal{N}_K(\mathbf{x}_i^B)$ is online efficiently computed with Approximate Nearest Neighbor Search [33], $s(\mathbf{x}_i^B, \tilde{\mathbf{x}}_j^B)$ can be computed with a complexity of $O(K)$ using the reverse mapping. Once $\tilde{\mathcal{X}}_i^B$ is chosen, the corresponding training pairs $\tilde{\mathcal{X}}_i = \{(\tilde{\mathbf{x}}_{i_1}^A, \tilde{\mathbf{x}}_{i_1}^B), \ldots, (\tilde{\mathbf{x}}_{i_{K_i}}^A, \tilde{\mathbf{x}}_{i_{K_i}}^B)\}$ are obtained since the correspondences of training samples are known. In practice, one training sample $\tilde{\mathbf{x}}_j^B$ may correspond to multiple training samples in camera view A and more training pairs are obtained. In order to simplify the description, we assume that $\tilde{\mathbf{x}}_j^B$ only has one corresponding sample in another camera view without affecting the generalization of the proposed algorithm.

Each training pair $(\tilde{\mathbf{x}}_{i_j}^A, \tilde{\mathbf{x}}_{i_j}^B)$ is assigned with a weight w_{ij} according to its visual similarities with the candidate sample $\mathbf{x}_i^B$ and the query sample $\mathbf{x}_q^A$. A training pair with a larger weight will have larger contribution for learning the adaptive metric. w_{ij} is defined as following,

$$w_{ij} = w_{ij}^B \cdot w_{ij}^A, \tag{2}$$

[1] In our implementation $K = 10$.

$$w_{ij}^B = exp\left(-\frac{\|\mathbf{x}_i^B - \tilde{\mathbf{x}}_{i_j}^B\|_2^2}{2\sigma_i^2}\right), \tag{3}$$

$$w_{ij}^A = exp\left(-\frac{\|\mathbf{x}_q^A - \tilde{\mathbf{x}}_{i_j}^A\|_2^2}{2\sigma_0^2}\right), \tag{4}$$

where $\sigma_i^2 = \text{median}(\{\|\mathbf{x}_i^B - \tilde{\mathbf{x}}_{i_j}^B\|_2^2\}_{\tilde{\mathbf{x}}_{i_j}^B \in \tilde{\mathcal{X}}_i^B})$ and $\sigma_0^2 = \text{median}(\{\|\tilde{\mathbf{x}}_i^A - \tilde{\mathbf{x}}_j^A\|_2^2\}_{\tilde{\mathbf{x}}_i^A, \tilde{\mathbf{x}}_j^A \in \mathcal{S}})$. w_{ij}^B is straightforward, since the selected training samples are supposed to be visually similar to the candidates. w_{ij}^A has two purposes. (1) Even though some selected samples are similar with the candidate in camera B, their samples observed in camera A may be dissimilar with the query sample, because of pose variations. It is not useful to learn the adaptive metric from such training pairs, since their inter-camera variations are different than that of the query person. The learned adaptive metric is supposed to depress the inter-camera variation of the query person. (2) If the selected training samples are similar to $\mathbf{x}_q$ in camera A, their corresponding candidate persons are easy to be confused with the query person. Therefore, we should give more weights to their training samples to well distinguish them in transfer learning. Some examples are shown in Figure 2. $\{w_{2j}^A\}$ of the samples in $\tilde{\mathcal{X}}_2$ are low because their observations in A have very different colors than the query sample and the second candidate can be easily distinguished from the query person. $\{w_{3j}^A\}$ of the samples in $\tilde{\mathcal{X}}_3$ are also low because their pose variations are different than that of the query person. The inter-camera variation of the query person is not well captured by the training samples in $\tilde{\mathcal{X}}_3$. Both $\{w_{1j}^A\}$ and $\{w_{4j}^A\}$ have large weights because the first and the fourth candidates are similar to the query person and therefore a metric needs to be specially trained to extract their subtle differences. Also the inter-camera variations existing in $\tilde{\mathcal{X}}_1$ and $\tilde{\mathcal{X}}_4$ well match with that of the query person.

3.3 Learning adaptive metrics by maximizing weighted margins

Given a positive semidefinite (PSD) matrix M, the distance between two samples $\mathbf{x}_i^A$ and $\mathbf{x}_j^B$ observed in two different camera views is computed as

$$d(\mathbf{x}_i^A, \mathbf{x}_j^B) = (\mathbf{x}_i^A - \mathbf{x}_j^B)^t M (\mathbf{x}_i^A - \mathbf{x}_j^B). \tag{5}$$

We first learn a generic metric M_0 from the whole training set $\mathcal{S}$. Given a query sample $\mathbf{x}_q$, its candidate set $\mathcal{X}_c^B$ and the selected training pairs $\{\tilde{\mathcal{X}}_i\}_{i=1}^N$, an adaptive metric M is learned with a regularization added by M_0. It minimizes the following objective function with constraints,

$$\min \quad \|M - M_0\|_F^2 + C \sum w_{ij} \cdot w_{i'j'} \cdot \xi_{iji'j'}, \tag{6}$$

$$s.t. \quad (\tilde{\mathbf{x}}_{i_j}^A - \tilde{\mathbf{x}}_{i'_{j'}}^B)^t M (\tilde{\mathbf{x}}_{i_j}^A - \tilde{\mathbf{x}}_{i'_{j'}}^B) - (\tilde{\mathbf{x}}_{i_j}^A - \tilde{\mathbf{x}}_{i_j}^B)^t M (\tilde{\mathbf{x}}_{i_j}^A - \tilde{\mathbf{x}}_{i_j}^B)$$

$$\geq 1 - \xi_{iji'j'} \qquad \forall i, j, i', j', i \neq i' \tag{7}$$

$$M \succeq 0, \xi_{iji'j'} \geq 0 \tag{8}$$

Algorithm 1: Learning an adaptive metric for each candidate set by optimizing (6-8) with the cutting plane method.

$\mathcal{W} = \emptyset$;
$M = M_0$;
$\xi_{iji'j'} = 0$;
begin
  repeat
    $(\hat{i}, \hat{j}, \hat{i}', \hat{j}') = \arg\max_{(i,j,i',j')} w_{ij} \cdot w_{i'j'}(1 - \psi_{iji'j'}(M))$;
    if $1 - \psi_{\hat{i}\hat{j}\hat{i}'\hat{j}'}(M) > \xi_{\hat{i}\hat{j}\hat{i}'\hat{j}'} + \epsilon$ **then**
      $\mathcal{W} = \mathcal{W} \cup \{(\hat{i}, \hat{j}, \hat{i}', \hat{j}')\}$;
      Solve the following QP problem using ADMM;
        $(M, \{\xi_{iji'j'}\}) = \arg\min ||M - M_0||_F^2 + C \sum_{iji'j'} w_{ij} \cdot w_{i'j'} \cdot \xi_{iji'j'}$
        $s.t.\ \forall (i, j, i', j') \in \mathcal{W}$
          $(\tilde{\mathbf{x}}^A_{i_j} - \tilde{\mathbf{x}}^B_{i'_{j'}})^t M (\tilde{\mathbf{x}}^A_{i_j} - \tilde{\mathbf{x}}^B_{i'_{j'}}) - (\tilde{\mathbf{x}}^A_{i_j} - \tilde{\mathbf{x}}^B_{i_j})^t M (\tilde{\mathbf{x}}^A_{i_j} - \tilde{\mathbf{x}}^B_{i_j}) \geq 1 - \xi_{iji'j'}$
          $M \succeq 0, \xi_{iji'j'} \geq 0$
  until $\mathcal{W}$ *does not change*;

The distance between two metrics is define as

$$\|M - M_0\|_F^2 = \sum_{ij} (M[i,j] - M_0[i,j])^2 = \mathbf{tr}((M - M_0)(M - M_0)^t). \quad (9)$$

$(\tilde{\mathbf{x}}^A_{i_j} - \tilde{\mathbf{x}}^B_{i_j})^t M (\tilde{\mathbf{x}}^A_{i_j} - \tilde{\mathbf{x}}^B_{i_j})$ is the distance between two samples of the same person (i, j) observed in different camera views under the metric M. It is supposed to be smaller than any $(\tilde{\mathbf{x}}^A_{i_j} - \tilde{\mathbf{x}}^B_{i'_{j'}})^t M (\tilde{\mathbf{x}}^A_{i_j} - \tilde{\mathbf{x}}^B_{i'_{j'}})$, which is the distance between the samples of (i, j) and a different person (i', j'), with a margin. The slack penalties are weighted with w_{ij} and $w_{i'j'}$. Here we require that $i \neq i'$. If $i = i'$, the two selected training persons (i, j) and (i, j') are actually related to the same candidate and we do not have to distinguish them.

Our objective function (6) is convex with liner constraints,

$$\begin{aligned}
\psi_{iji'j'}(M) &= (\tilde{\mathbf{x}}^A_{i_j} - \tilde{\mathbf{x}}^B_{i'_{j'}})^t M (\tilde{\mathbf{x}}^A_{i_j} - \tilde{\mathbf{x}}^B_{i'_{j'}}) - (\tilde{\mathbf{x}}^A_{i_j} - \tilde{\mathbf{x}}^B_{i_j})^t M (\tilde{\mathbf{x}}^A_{i_j} - \tilde{\mathbf{x}}^B_{i_j}) \\
&= \mathbf{tr}(M (\tilde{\mathbf{x}}^A_{i_j} - \tilde{\mathbf{x}}^B_{i'_{j'}})(\tilde{\mathbf{x}}^A_{i_j} - \tilde{\mathbf{x}}^B_{i'_{j'}})^t) - \mathbf{tr}(M (\tilde{\mathbf{x}}^A_{i_j} - \tilde{\mathbf{x}}^B_{i_j})(\tilde{\mathbf{x}}^A_{i_j} - \tilde{\mathbf{x}}^B_{i_j})^t) \\
&\geq 1 - \xi_{iji'j'}. \qquad (10)
\end{aligned}$$

It can be solved by Semidefinite Programming (SDP). We did not choose the subgradient method [34], which has been used by many metric learning approaches [35], to solve this optimization problem, because it simultaneously considers all the constraints and the computational cost is high. Instead, we adopt the cutting plane method [36] and our learning steps are summarized in Algorithm (1). Since M is initialized with M_0 which is a reasonably good starting point, only a small portion of samples violate the constraints of (7) during the optimization process.

At each of the iterative steps, we choose samples with the largest violation of the constraint of margin,

$$(\hat{i}, \hat{j}, \hat{i}', \hat{j}') = \underset{(i,j,i',j')}{\arg\max}\ w_{ij} \cdot w_{i'j'}(1 - \psi_{iji'j'}(M)), \tag{11}$$

and add them to a working set $\mathcal{W}$[2]. Then M and $\{\xi_{iji'ji}\}$ are optimized only considering the constraints added by the samples in $\mathcal{W}$. The objective function (6) is quadratic in M and linear in $\xi_{iji'j'}$, and can be solved using Quadratic Programming (QP). We implement the QP solver using the Alternating Direction Method of Multipliers (ADMM) [37][3] which was proven to have a fast convergence rate. Our optimization procedure is inspired by structural SVM [20] where the cutting plane method was also used and it converged fast. The convergence of our algorithm is guaranteed, since $\mathcal{W}$ cannot increase forever. The convergence rate of our algorithm is controlled by ϵ and a global optimal with ϵ violation of margin is obtained. Asymptotically, with $\epsilon \to 0$, the global optimal can be obtained. According to the suggestions of [20], we choose $\epsilon = 0.001$. The parameter C is chosen as $1/\text{mean}(\{\|\tilde{\mathbf{x}}_i - \tilde{\mathbf{x}}_j\|_2^2\}_{\tilde{\mathbf{x}}_i, \tilde{\mathbf{x}}_j \in \mathcal{S}})$ referring to the recommendation of SVMLight[4].

From (2-4) and (6-8) it is observed that if a query sample and its candidate set are dissimilar with any samples in the training set, few training samples are selected and their weights are small. In that case, there are few constraints and the adaptive metric M is very close to generic metric M_0. **Learning the generic metric.** M_0 is learned by minimizing the following objective function,

$$\begin{aligned} \min \quad & \|M_0\|_F^2 + C\sum_{i,j}\xi_{ij}, \\ s.t. \quad & (\tilde{\mathbf{x}}_i^A - \tilde{\mathbf{x}}_j^B)^t M_0(\tilde{\mathbf{x}}_i^A - \tilde{\mathbf{x}}_j^B) - (\tilde{\mathbf{x}}_i^A - \tilde{\mathbf{x}}_i^B)^t M_0(\tilde{\mathbf{x}}_i^A - \tilde{\mathbf{x}}_i^B) \geq 1 - \xi_{ij}, \forall i,j, i \neq j \\ & M_0 \succeq 0, \xi_{iji'j'} \geq 0 \end{aligned} \tag{12}$$

All the samples in the whole training set are included. $(\tilde{\mathbf{x}}_i^A, \tilde{\mathbf{x}}_i^B)$ are the training samples of the same person observed in different camera views, and $(\tilde{\mathbf{x}}_i^A, \tilde{\mathbf{x}}_j^B)$ are the training samples of different persons. Once M_0 is learned, it is normalized by $M_0 = \frac{M_0}{\mathbf{tr}(M_0)}$.

4 Experimental Results

4.1 Dataset Description

Experiments are conducted on the VIPeR dataset [21] and the *Campus*[5] dataset built by us. The VIPeR dataset is a widely used benchmark for evaluating human

[2] $\mathcal{W}$ is initialized as empty and no samples are removed from $\mathcal{W}$ during the optimization procedure.

[3] In ADMM, after each gradient step, the updated M is projected back onto the feasible set of PSD matrices by spectral decomposition.

[4] `http://svmlight.joachims.org/`

[5] `http://www.ee.cuhk.edu.hk/~xgwang/CUHK_identification.html`

(a) VIPeR

(b) Campus

Fig. 3. Examples of images from the VIPeR dataset and the Campus dataset.

reidentification algorithms. It includes 632 persons captured in two camera views. Each person has one image per camera view. The Campus dataset has 971 persons and each person also has two images captured in two disjoint camera views. Some examples of images from the two datasets are shown in Figure 3. Large inter-camera variations are observed in both datasets, which makes human reidentification challenging. The VIPeR dataset is even more challenging because even in the same camera view, persons appear in different poses and viewpoints, and lighting and background also change. It is difficult to learn a single generic metric to depress many kinds of inter-camera variations. In the Campus dataset, camera B mainly includes images of the frontal view and the back view, and camera A has more variations of viewpoints and poses.

4.2 Generic metric learning

We first test our generic metric learning algorithm, i.e., learning M_0 by minimizing (12), and compare it with other metric learning algorithms and the state-of-the-art human reidentification algorithms. The accumulative recognition accuracies on the VIPeR and Campus datasets are shown in Figure 4. For each of them, 50% persons are randomly selected for training and the remaining ones are used for testing. The random partition is repeated for ten times

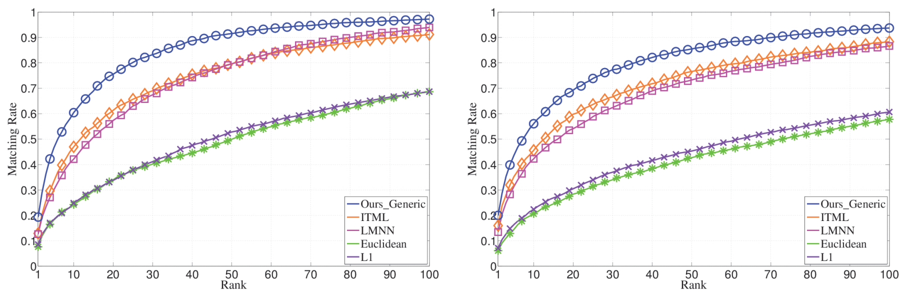

(a) VIPeR (b) Campus

Fig. 4. Evaluate the performance of generic metric learning on the whole gallery set without using temporal reasoning to prune the candidates. See details in Section 4.2.

and the average accuracies are computed. It is assumed that temporal reasoning is not used and each query sample matches the object from the whole gallery set. This is the scenario all the existing human reidentification algorithms assumed. We compare with two state-of-the-art metric learning algorithms, Large Margin Nearest Neighbor Classification (LMNN) [35] and Information-Theoretic Metric Learning (ITML) [38], as well as directly matching visual features with Euclidean distance (Euclidean) and L_1 distance (L_1). Our learned generic metric (Ours_Generic) has a better performance. Its rank-one accuracy is 19.3% on the VIPeR dataset. Some other state-of-the-art human reidentification techniques with different visual features and learning algorithms were also evaluated on the VIPeR dataset and published in literature with the same gallery size and in the same way of randomly partitioning the dataset [4]. The highest rank one accuracy reported so far is 15.66% [4]. Since their implementations are not available, we do not have their results on the Campus dataset. Compared to PRDC in [4], our methods enjoy a global optimal solution. Compared with ITML, our generic metric learning method employs a relative distance comparison rather than a hard global threshold between negative and positive pairs. For LMNN, as the distance is measured cross domain, the initial neighborhood selection will probability have no samples from the same identity selected which will bias the whole optimization procedure. Our generic metric learning algorithm for human reidentification is at least comparable with the state-of-the-art. However, this is **not** the main contribution of our framework. We focus on transferred metric learning.

4.3 Transferred metric learning

In this experiment, it is assumed that temporal reasoning can prune candidates and therefore for each query image the size of the candidate set could be much smaller than the gallery size. We have tried different sizes (N) of candidate sets from 5 to 50. The partitioning of training/test subsets is in the same way as Section 4.2. We design our experiment to simulate the real world scenario by random sampling the query-candidate configuration based on the assumption

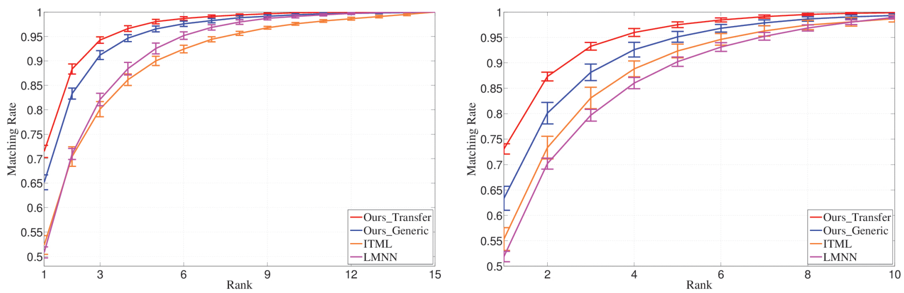

(a) VIPeR (b) Campus

Fig. 5. Average accumulative recognition accuracies and their standard deviations on the candidate sets. The size of the candidate sets is fixed as 15. The bars indicate standard deviations

that appearance is independent of the temporal reasoning. In order to validate our approach with a wide variety of configurations, for each query sample in the test set, we randomly select $N-1$ samples observed in the other camera view from the test set and also select the truly matched sample to form its candidate set. The same experimental design was also adopted in [3]. Human reidentification is to recognize the right person from the N candidates. For each query image, this process is repeated for 50 times given a fixed training/test data partition. The partition of training/test data is repeated for 10 times. When the size of candidate sets is fixed as 15, the average accumulative recognition accuracies and their standard deviations on the two datasets are shown in Figure 5. Our transferred metric learning (Ours_Transferred) clearly outperforms our generic metric learning as well as other generic metric learning algorithms such as ITML and LMNN. The rank-one accuracy has been improved by 6.32% and 9.71% on the VIPeR dataset and the Campus dataset respectively. With an unoptimized matlab implementation and on a Core 8 2.27GHz CPU, it takes less than two seconds to train an adaptive metric for a candidate set of size 15. Figure 6 plots the average rank-one accuracies and their standard deviations when the size (N) of the candidate sets varies from 5 to 50. When N is small, the generic metric performs well and the improvement of the transferred metric learning is relatively small. When N is too large (> 50), the distributions of samples in the candidate set is complicated and close to the global distribution of the whole training set. In this case, the idea of adapting the metric to a local region of the training set is not feasible any more and most training samples are selected as the neighbors of the candidate set. Therefore, the learned adaptive metric is similar to the generic metric and the improvement becomes little. Compared with figure 4(b) in [3], the settings are same to ours and our approach outperforms the result test using the manually designed feature in VIPeR benchmark dataset with all candidate set size reported in their paper. The size of the training set is an important factor affecting the effectiveness of transfer learning. When the training set is large, it is more likely for the candidates to find similar training samples. Figure

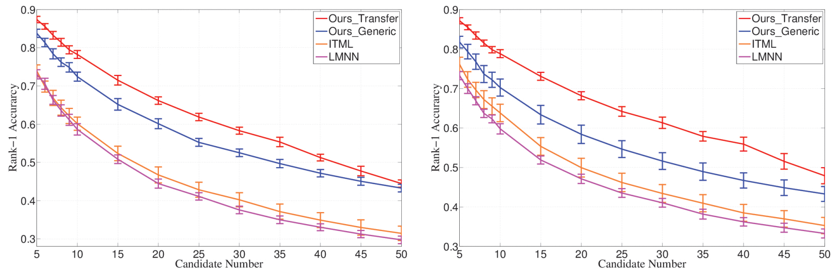

(a) VIPeR (b) Campus

Fig. 6. Average rank-one accuracies when size of candidate sets varies from 5 to 50.

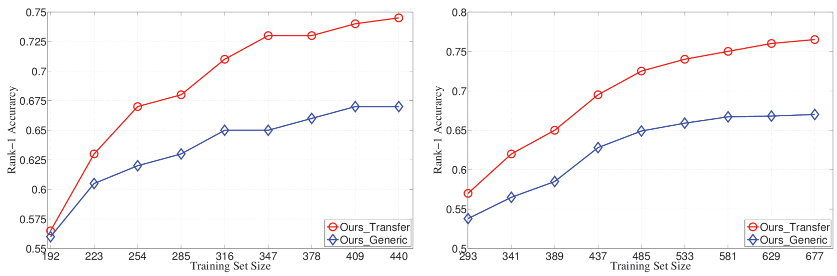

(a) VIPeR (b) Campus

Fig. 7. Average rank-one accuracies when the size of the training set changes.

7 plots the average rank-one accuracies when the size of the training set changes. When the training set gets large, the difference between the transferred metric learning and generic metric learning becomes large.

5 Conclusions and Discussions

In this paper, we solve the human reidentification problem from a new angle. Instead of trying to learn a generic metric to distinguish all the persons and to depress all types of inter-camera variations, we learn an adaptive metric for a specific candidate set under the framework of transfer learning. Given a query sample and its candidate set, the samples in the training set are selected and reweighted. An adaptive metric is learned by maximizing weighted margin of the selected training samples and being regularized by a generic metric. Experiments on the widely used VIPeR dataset and our Campus dataset shows that transferred metric learning is more effective than generic metric learning on human reidentification.

In this paper, we assume that the samples are from two fixed camera views. But the proposed approach also has good potentials to be generalized to the case when training and testing sets have multiple camera views or even the case when training and testing data are taken with different cameras. In the VIPeR dataset, persons captured by the same camera show a large diversity on poses, viewpoints, lightings and background. It is close to the general case of more camera views. In our approach, the training samples are selected and weighted by matching the visual features with the test samples. Therefore, the selected training samples should well match the query sample and candidate samples in pose, viewpoint and lighting even though they may be taken by different cameras. In the future work, we will build a new dataset with diversified camera views and will further improve our approach to make it work in more general camera settings.

6 Acknowledgment

This work is supported by the General Research Fund sponsored by the Research Grants Council of Hong Kong (project No. CUHK417110 and CUHK417011) and National Natural Science Foundation of China (project no. 61005057).

References

1. Gheissari, N., Sebastian, T.B., Rittscher, J., Hartley, R.: Person reidentification using spatiotemporal appearance. In: CVPR. (2006)
2. Schwartz, W., Davis, L.: Learning discriminative appearance-based models using partial least sqaures. In: Proc. XXII SIBGRAPI. (2009)
3. Farenzena, M., Bazzani, L., Perina, A., Murino, V., Cristani, M.: Person re-identification by symmetry-driven accumulation of local features. In: CVPR. (2010)
4. Zheng, W., Gong, S., Xiang, T.: Person re-identification by probabilistic relative distance comparison. In: CVPR. (2011)
5. Park, U., Jain, A., Kitahara, I., Kogure, K., Hagita, N.: Vise: Visual search engine using multiple networked cameras. In: ICPR. (2006)
6. Weijer, J., Schmid, C.: Coloring local feature extraction. In: ECCV. (2006)
7. Dalal, N., Triggs, B.: Histograms of oriented gradients for human detection. In: CVPR. (2005)
8. Wang, X., Doretto, G., Sebastian, T., Rittscher, J., Tu, P.: Shape and appearance context modeling. In: ICCV. (2007)
9. Daugman, J.G.: Uncertainty relation for resolution in space, spatial frequency, and orientation optimized by two-dimensional visual cortical filters. Journal of the Optical Society of America A **2** (1985) 1160–1169
10. Ojala, T., Pietikäinen, M., Mäenpää, T.: Multiresolution gray-scale and rotation invariant texture classification with local binary patterns. IEEE Trans. on PAMI (2002) 971–987
11. Torralba, A., Murphy, K., Freeman, W., Rubin, M.: Context-based vision system for place and object recognition. In: ICCV. (2003)
12. Porikli, F.: Inter-camera color calibration by correlation model function. In: ICIP. (2003)
13. Javed, O., Shafique, K., Shah, M.: Appearance modeling for tracking in multiple non-overlapping cameras. In: CVPR. (2005)
14. Gilbert, A., Bowden, R.: Tracking objects across cameras by incrementally learning inter-camera colour calibration and patterns of activity. In: ECCV. (2006)
15. Prosser, B., Gong, S., Xiang, T.: Multi-camera matching using bi-directional cumulative brightness transfer function. In: BMVC. (2008)

16. Gray, D., Tao, H.: Viewpoint invariant pedestrian recognition with an ensemble of localized features. In: ECCV. (2008)
17. Shan, Y., Sawhney, H., Kumar, R.: Unsupervised Learning of Discriminative Edge Measures for Vehicle Matching between Nonoverlapping Cameras. Pattern Analysis and Machine Intelligence, IEEE Transactions on **30** (2008) 700–711
18. Lin, Z., Davis, L.: Learning pairwise dissimilarity profiles for appearance recognition in visual surveillance. In: Proc. Int'l Symposium on Advances in Visual Computing. (2008)
19. Prosser, B., Zheng, W., Gong, S., Xiang, T., Mary, Q.: Person re-identification by support vector ranking. In: BMVC. (2010)
20. Tsochantaridis, I., Joachims, T., Hofmann, T., Altun, Y.: Large margin methods for structured and interdependent output variables. Journal of Machine Learning Research **6** (2005) 1453–1484
21. Gray, D., Brennan, S., Tao, H.: Evaluating appearance models for recognition, reacquisition, and tracking. (2007)
22. Dai, W., Yang, Q., Xue, G., Yu, Y.: Boosting for transfer learning. In: Proc. of ICML. (2007)
23. Wu, X., Srihari, R.: Incorporating prior knowledge with weighted margin support vector machines. In: Proc. of SIGKDD. (2004)
24. Jiang, W., Zavesky, E., Chang, S., Loui, A.: Cross-domain learning methods for high-level visual concept classification. In: ICIP. (2008)
25. Saenko, K., Kulis, B., Fritz, M., Darrell, T.: Adapting visual category models to new domains. In: ECCV. (2010)
26. Yao, Y., Doretto, G.: Boosting for transfer learning with multiple sources. In: CVPR. (2010)
27. Qi, G., Aggarwal, C., Huang, T.: Towards semantic knowledge propagation from text corpus to web images. In: Proc. of WWW. (2011)
28. Yang, J., Yan, R., Hauptmann, A.G.: Cross-domain video concept detection using adaptive svms. In: Proc. of ACM Multimedia. (2007)
29. Duan, L., Tsang, I.W., Xu, D., Maybank, S.J.: Domain transfer svm for video concept detection. In: CVPR. (2009)
30. Qi, G., Aggarwal, C., Rui, Y., Tian, Q., Chang, S., Huang, T.: Towards cross-category knowledge propagation for learning visual concepts. In: CVPR. (2011)
31. Zhan, D.C., Li, M., Li, Y.F., Zhou, Z.H.: Learning instance specific distances using metric propagation. In: Proc. of ICML. (2009) 154
32. Sande, K., Gevers, T., Snoek, C.G.M.: Evaluating color descriptors for object and scene recognition. IEEE Trans. on PAMI **32** (2010) 1582–1596
33. Liu, T., Moore, A.W., Gray, A.G., Yang, K.: An investigation of practical approximate nearest neighbor algorithms. In: Proc. of NIPS. (2004)
34. Fletcher, R.: Semi-definite matrix constraints in optimization. SIAM J. Control Optim. **23** (1985) 493–513
35. Weinberger, K.Q., Saul, L.K.: Distance metric learning for large margin distance metric learning for large margin. Journal of Machine Learning Research **10** (2009) 207–244
36. Luenberger, D., Ye, Y.: Linear and Nonlinear Programming. Springer Verlag (2008)
37. Boyd, S., Parikh, N., Chu, E., Peleato, B., Eckstein, J.: Distributed optimization and statistical learning via the alternating direction method of multipliers. Foundations and Trends in Machine Learning **3** (2011) 1–122
38. Davis, J.V., Kulis, B., Jain, P., Sra, S., Dhillon, I.S.: Information-theoretic metric learning. In: Proc. of ICML. (2007)